

Improved Transient Simulation of Salient-Pole Synchronous Generators With Internal and Ground Faults in the Stator Winding

Daqiang Bi, Xiangheng Wang, Weijian Wang, Z. Q. Zhu, *Senior Member, IEEE*, and David Howe

Abstract—An improved model for simulating the transient behavior of salient-pole synchronous generators with internal and ground faults in the stator winding is established using the multiloop circuit method. The model caters for faults under different ground conditions for the neutral, and accounts for the distributed capacitances of the windings to ground. Predictions from the model are validated by experiments, and it is shown that the model accurately predicts the voltage and current waveforms under fault conditions. Hence, it can be used to analyze important features of faults and to design appropriate protection schemes.

Index Terms—Ground fault, internal fault, multiloop circuit method, salient-pole generator.

NOMENCLATURE

i	Current.
p	Differential operator d/dt .
u	Voltage.
ψ	Flux-linkage.
M	Mutual-inductance.
L	Self-inductance.
R, r	Resistance.
C	Capacitance.

Subscripts

a, b, c	Three-phase windings.
k	Branch k per phase ($k = 1 \sim m$).
j	Segment j per branch ($j = 1 \sim s$).
d	Damping winding.
g	Damping winding loop ($g = 1 \sim h$).
f	Field winding.
t	Terminal.
n	Neutral.
P	Potential transformer.

I. INTRODUCTION

AS THE capacity of single generators in power systems becomes larger, their protection becomes evermore critical, since the large transient short-circuit current which may result with internal faults can cause catastrophic damage, while ground faults, which may be only slightly destructive during their initial stages, may, in the long term, develop into internal

short-circuit faults. Therefore, appropriate protection schemes must be employed to cater for both internal and ground faults. Hence, a comprehensive simulation model is required to analyze the characteristics of such faults and to accurately predict the associated voltage and current waveforms.

Several methods for analyzing the effect of internal faults in synchronous generators have been proposed [1]–[7]. Strong space harmonics exist in the air-gap magnetic field and significant time harmonics exist in the phase currents due to the resulting asymmetry in the stator windings. Hence, the symmetrical component method which was employed in [1], [2] can lead to significant errors. Direct phase quantities were used in [3], [4] to study the effect of internal faults, including internal faults between turns and the neutral of the stator winding. It was assumed that the winding inductances relative to the air-gap field were proportional to the product of the effective numbers of turns of the corresponding windings. However, this is correct only when the air-gap field has a fundamental component or if the windings are concentrated. A direct phase representation was also used in [5]–[7], and a unique winding partition technique was employed to analyze internal faults. A winding with an internal fault was divided into two sub-windings, each being treated as an equivalent sinusoidally distributed winding. However, space harmonics in the air-gap field were neglected and no experimental validation was provided.

To date, the analysis of ground faults has focused mainly on the characteristics of the zero-sequence fundamental and third-harmonic voltage components by using equivalent circuits. However, since the distribution of the third-harmonic voltage of each coil in different branches of the stator winding may be different, the equivalent circuits for turbo-generators presented in [8]–[10] cannot be applied to salient-pole generators. For a salient-pole generator with multiple branches, the analysis of the third-harmonic voltage generally adopts the superposition principle based on the potential of each turn [11], the fundamental and third-harmonic components being calculated independently. However, this is not always valid in practice and, hence, the utility of the simulation model is limited.

Although several machine models are employed in commercial software for the analysis of power systems, such as EMTP [12] and EMTDC [13], the generators are generally considered as healthy units, and the software is not capable of analyzing the effect of internal and ground faults.

The basic principle of the multiloop circuit method developed in [14] and [15] is to generate equations for the voltages and flux-linkages according to the actual circuit loops of the

Manuscript received October 23, 2003. Paper no. TEC-00152-2003.

D. Bi, X. Wang, and W. Wang are with the Department of Electrical Engineering and Applied Electronic Technology, Tsinghua University, Beijing 100084, China (e-mail: bidaqiang@mail.tsinghua.edu.cn).

Z. Q. Zhu and D. Howe are with the Department of Electronic and Electrical Engineering, University of Sheffield, Sheffield S1 3JD, U.K.

Digital Object Identifier 10.1109/TEC.2004.841509

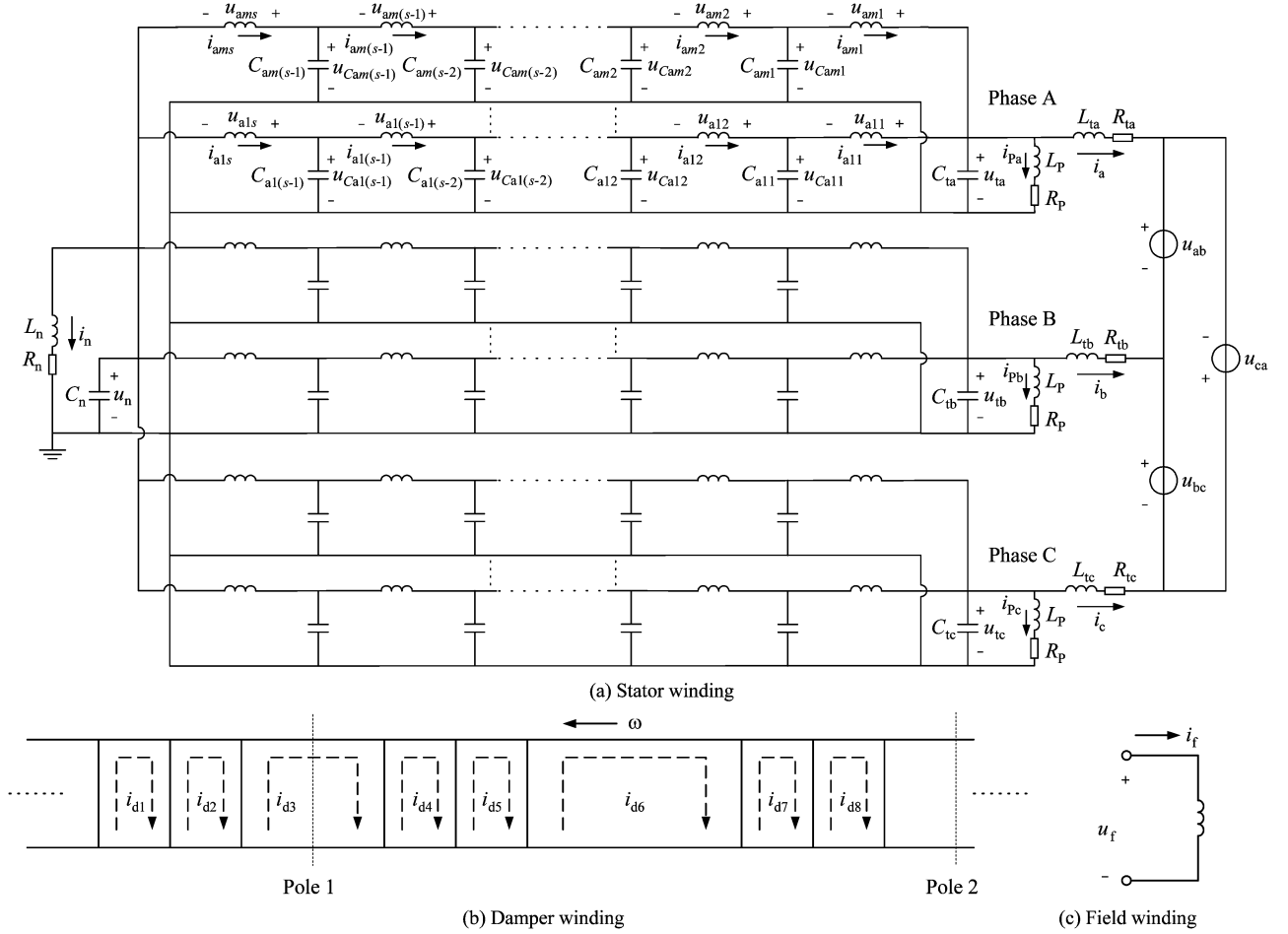


Fig. 1. Simulation model for fault on stator winding of salient-pole generator.

machine, using appropriate circuit parameters. The method has been verified by experiments, and shown to be capable of analyzing the steady-state and transient behavior of internal faults in the stator windings of synchronous generators [16], [17] since it accounts for the actual disposition of the windings and accurately calculates the harmonics in the air-gap field. However, since the distributed capacitances of the windings to ground are neglected, while the grounding method for the neutral is not considered, ground faults could not be simulated and analyzed. Therefore, the aim of this paper is to extend the multi-loop circuit method to cater for both internal and ground faults under different neutral ground conditions and to account for the distributed capacitances of the windings to ground.

II. ANALYTICAL MODEL BASED ON MULTILoop CIRCUIT METHOD

A. Definition of Reference Direction

For the stator winding shown in Fig. 1(a), the generator rule is adopted and positive current produces a negative flux-linkage. For the rotor windings, i.e., both the field winding and the damper winding shown in Fig. 1(b) and (c), the motor rule is adopted and positive current produces a positive flux-linkage. Positive voltage drops and current polarities in the stator and

rotor windings, as well as positive voltage drops across the capacitances, the neutral grounding resistance R_n and inductance L_n , and the voltage transformer parameters L_P and R_P at the generator terminals, are also indicated in Fig. 1.

B. Division of Distributed Capacitance

Each stator phase winding is composed of m branches in parallel, and each branch consists of n coils in series. Assuming that C_a , C_b , and C_c , the capacitances of phases a , b and c to ground, respectively, are evenly distributed in the winding, then the capacitance of each coil of phases a , b and c is $C_{a1} = C_a/(mn)$, $C_{b1} = C_b/(mn)$ and $C_{c1} = C_c/(mn)$, respectively. In the model, every branch is divided into s segments from the terminal to the neutral, and the j th segment includes w_j coils (where $\sum_{j=1}^s w_j = n$). The distributed capacitance of each segment of the winding is replaced by two equal lumped capacitances at both ends. At the terminals, the additional capacitances of phases a , b , and c , viz. the equivalent capacitances between the terminals and the low-voltage winding of the step-up transformer are C_{t1} , C_{t2} , and C_{t3} , respectively. Thus, in the stator model, the equivalent capacitances can be expressed as follows: at the terminals $C_{ta} = mw_1C_{a1}/2 + C_{t1}$, $C_{tb} = mw_1C_{b1}/2 + C_{t2}$, and $C_{tc} = mw_1C_{c1}/2 + C_{t3}$; inside the stator winding $C_{akj} = C_{a1}(w_j + w_{j+1})/2$, $C_{bkj} = C_{b1}(w_j + w_{j+1})/2$, and $C_{ckj} = C_{c1}(w_j + w_{j+1})/2$, ($k = 1 \sim m$, $j = 1 \sim s - 1$); at the neutral $C_n = mw_s(C_{a1} + C_{b1} + C_{c1})/2$.

If the resistance of each coil is r_1 , then the resistance of each segment per phase and branch is $r_{akj} = r_{bkj} = r_{ckj} = w_j r_1$ ($k = 1 \sim m, j = 1 \sim s - 1$).

C. Establishment of State Equations

The currents through the inductances and the voltages across the capacitances are chosen as the state variables, and the state equations are established for both healthy and fault states.

In the following, the equivalent resistances and inductances of phases a, b , and c from the terminals to the infinite bus, including the step-up transformer and the transmission line, are R_{ta}, R_{tb}, R_{tc} , and L_{ta}, L_{tb}, L_{tc} , respectively. The calculation of the winding inductances has been described in detail in [15] and [16]. It is worth mentioning that for a salient-pole generator, the self- and mutual-inductance between segments of the stator winding, and the mutual-inductance between the stator and rotor windings are dependent on the angular position of the rotor; while the self- and mutual-inductances of the rotor windings are independent of the angular position of the rotor.

1) Healthy State:

a) *Voltage Equations of Independent Loops:* The voltage equations for each segment of the stator winding can be expressed as shown in (1), at the bottom of the page, where the state variable vector is

$$\mathbf{I} = [i_{a11} \dots i_{ams}, i_{b11} \dots i_{bms}, i_{c11} \dots i_{cms}, i_{d1} \dots i_{dg} \dots i_{dh}, i_f]^T$$

and the inductance row vector of segment j of branch k of phase a is

$$\mathbf{M}_{akj} = [-M_{akja11} \dots -L_{akj} \dots -M_{akjams}, -M_{akjb11} \dots -M_{akjbms}, -M_{akjc11} \dots -M_{akjcms}, M_{akjd1} \dots M_{akjdg} \dots M_{akjdh}, M_{akjff}].$$

The inductance vectors of the winding segments of phases b and c are similar.

The voltage equations for internal loops of the stator winding are as shown in (2), at the bottom of the page, where

$$\begin{aligned} u_{Cak0} &= u_{ta}, & u_{Cbk0} &= u_{tb}, \\ u_{Cck0} &= u_{tc}, & u_{Caks} &= u_{Cbks} = u_{Ccks} = u_n. \end{aligned}$$

The voltage equations of the damper winding loops are

$$\begin{aligned} p\psi_{dg} + r_{dg}i_{dg} - r_d(i_{d(g-1)} + i_{d(g+1)}) \\ = p(\mathbf{M}_{dgg}\mathbf{I}) + r_{dg}i_{dg} - r_d(i_{d(g-1)} + i_{d(g+1)}) = 0 \end{aligned} \quad (3)$$

where r_{dg} is the resistance of damper loop g ($g = 1 \sim h$), h is the number of damper loops, and r_d is the resistance of one damper bar ($i_{d0} = i_{dh}, i_{d(h+1)} = i_{d1}$).

The inductance row vector of loop g of the damper winding is

$$\mathbf{M}_{dg} = [-M_{dga11} \dots -M_{dgams}, -M_{dgb11} \dots -M_{dgbms}, -M_{dgc11} \dots -M_{dgcms}, M_{dgd1} \dots L_{dg} \dots M_{dgdh}, M_{dgff}].$$

The inductance vectors of other damper winding loops are similar. The voltage equation of the field winding loop is

$$u_f - p\psi_f - r_f i_f = u_f - p(\mathbf{M}_f \mathbf{I}) - r_f i_f = 0 \quad (4)$$

where r_f is the resistance of the field winding.

The inductance vector of the field winding is

$$\mathbf{M}_f = [-M_{fa11} \dots -M_{fams}, -M_{fb11} \dots -M_{fbms}, -M_{fc11} \dots -M_{fcms}, M_{fd1} \dots M_{fdg} \dots M_{fdh}, L_f].$$

At the terminals, the voltage equations for the load loops are

$$\begin{cases} -u_{ta} + L_{ta}p i_a + R_{ta}i_a + u_{ab} - L_{tb}p i_b - R_{tb}i_b + u_{tb} = 0 \\ -u_{tb} + L_{tb}p i_b + R_{tb}i_b + u_{bc} - L_{tc}p i_c - R_{tc}i_c + u_{tc} = 0 \end{cases} \quad (5)$$

where u_{ab} and u_{bc} are the line voltages of the infinite bus.

For the loops of the voltage transformer, the voltage equations are

$$\begin{cases} L_P p i_{Pa} + R_P i_{Pa} - u_{ta} = 0 \\ L_P p i_{Pb} + R_P i_{Pb} - u_{tb} = 0 \\ L_P p i_{Pc} + R_P i_{Pc} - u_{tc} = 0 \end{cases} \quad (6)$$

where L_P and R_P are the magnetizing inductance and resistance, respectively, of the voltage transformer at the generator terminals.

For the neutral loop, the voltage equation is

$$-L_n p i_n - R_n i_n + u_n = 0. \quad (7)$$

b) *Node Current Equations:* At the internal nodes of the stator, the current equations are shown in (8), at the bottom of the next page.

$$\begin{cases} u_{akj} = p\psi_{akj} - r_{akj}i_{akj} = p(\mathbf{M}_{akj}\mathbf{I}) - r_{akj}i_{akj} \\ u_{bkj} = p\psi_{bkj} - r_{bkj}i_{bkj} = p(\mathbf{M}_{bkj}\mathbf{I}) - r_{bkj}i_{bkj} \\ u_{ckj} = p\psi_{ckj} - r_{ckj}i_{ckj} = p(\mathbf{M}_{ckj}\mathbf{I}) - r_{ckj}i_{ckj} \end{cases} \quad (k = 1 \sim m, j = 1 \sim s) \quad (8)$$

and

$$\begin{cases} -u_{Caij} - u_{aij} + u_{Cai(j-1)} = 0 \\ -u_{Cbij} - u_{bij} + u_{Cbi(j-1)} = 0 \\ -u_{Ccij} - u_{cij} + u_{Cci(j-1)} = 0 \end{cases} \quad (k = 1 \sim m, j = 1 \sim s) \quad (9)$$

For the following state equation:

$$\begin{cases} \frac{d\mathbf{y}}{dt} = \mathbf{G}(\mathbf{y}, t) \\ \mathbf{y}(t_0) = \mathbf{y}_0 \end{cases}$$

the recursive relation in the Calahan method is given by

$$\mathbf{y}_{n+1} = \mathbf{y}_n + \frac{3}{4}\mathbf{K}_n + \frac{1}{4}\mathbf{L}_n$$

where

$$\begin{aligned} \mathbf{K}_n &= \Delta t \left[\mathbf{I} - \Delta t \cdot a_1 \left(\frac{\partial \mathbf{G}}{\partial \mathbf{y}} \right)_n \right]^{-1} \\ &\cdot \left[\mathbf{G}(\mathbf{y}_n, t_n) + a_1 \cdot \Delta t \left(\frac{\partial \mathbf{G}}{\partial t} \right)_n \right] \\ \mathbf{L}_n &= \Delta t \left[\mathbf{I} - \Delta t \cdot a_1 \left(\frac{\partial \mathbf{G}}{\partial \mathbf{y}} \right)_n \right]^{-1} \\ &\cdot \left[\mathbf{G}(\mathbf{y}_n + b_1 \cdot \mathbf{K}_n \cdot t_n, t_n + \Delta t \cdot b_1) \right. \\ &\quad \left. + a_1 \cdot \Delta t \left(\frac{\partial \mathbf{G}}{\partial t} \right)_n \right]. \end{aligned}$$

\mathbf{I} is a unit matrix, Δt is the calculation time step, $a_1 = 0.788675134595$, $b_1 = -1.15410053838$ [18].

By adopting a nonzero transition resistance, albeit very small, to simulate either a solid ground fault or an internal short-circuit fault, the Calahan method ensures good stability toward a solution.

IV. SIMULATION AND EXPERIMENTAL RESULTS

Extensive experiments, encompassing inter-turn faults in the same branch, faults between different branches in the same phase or between different phases, and ground faults, have been carried out on a salient-pole synchronous generator on no-load, with different excitation currents, and under different neutral grounding conditions. Some typical predicted and measured results will be reported in this section to demonstrate the generality and accuracy of the developed model. The main data for the experimental generator are: rated volt-amps = 15 kVA; rated power = 12 kW; rated voltage = 400 V; rated current = 21.7 A; excitation current on no-load and rated voltage = 8.24 A; number of pole-pairs = 2; number of parallel branches per phase = 2; number of coils per branch of stator phase winding = 7; number of damper bars per pole = 6; capacitances of stator phases a , b and c to ground = 2.01 nF, 1.96 and 2.11 nF, respectively. A tap from each coil of the stator winding exists in the experimental generator so as to enable the type of fault and its location to be selected. In the investigation, each branch is divided into seven segments from the terminal to the neutral.

A. Internal Fault

The excitation current was reduced to 2.85 A in order to avoid an excessively high fault current, while the neutral was grounded via a potential transformer. The measured and simulated short-circuit current i_g and excitation current i_f are compared in Fig. 4(a) and (b) when an inter-turn short-circuit fault

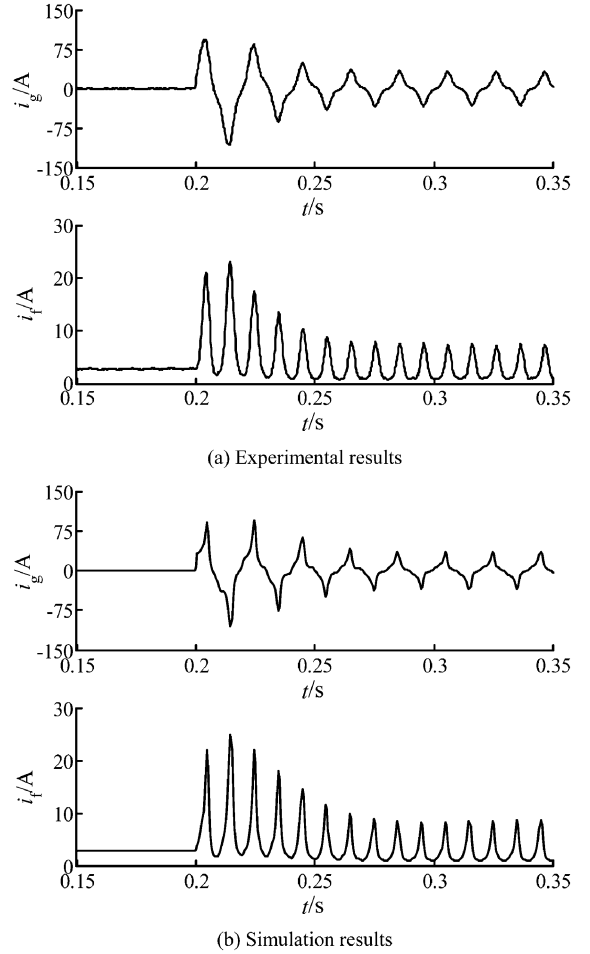


Fig. 4. Current waveforms with inter-turn fault.

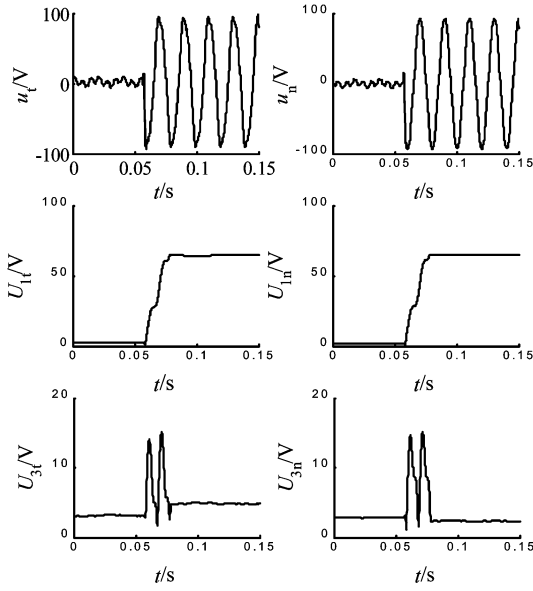
is imposed across coil 7 of branch 2 in the phase a winding, which is adjacent to the neutral point, when the transition resistance R_g is 0.95Ω . In general, it can be seen that the simulation results agree well with the experimental results.

Fig. 4 shows that the short-circuit current which results with an internal fault is very large, being nearly four times the rated current even with the reduced excitation current. Further, harmonic analysis shows that the distortion of the current waveforms is significant, the excitation current containing a strong second harmonic in addition to the direct current component, while the stator current contains a pronounced third harmonic.

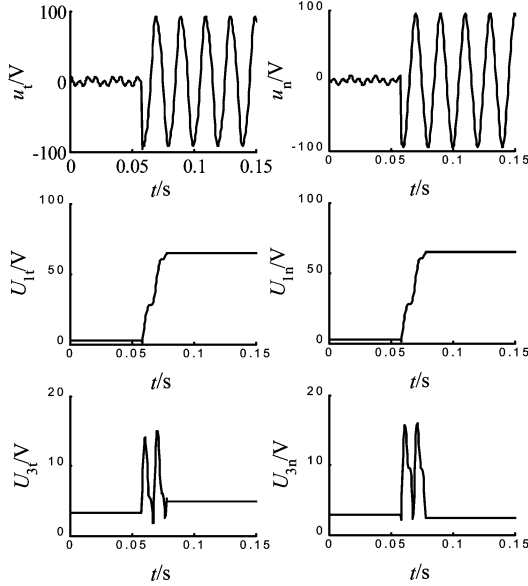
B. Ground Fault

The ground faults were applied with an excitation current of 7.7 A. Thus, the voltage between the terminals and ground was approximately equal to the rated phase voltage.

To verify the method of distributing the capacitance in the mathematical model, voltage waveforms were measured when a direct ground fault was applied on coil 2 of branch 1 in the phase a winding, while the neutral was ungrounded and there was no additional capacitance or voltage transformer at the terminals. The measured and simulated zero sequence voltages at the terminals and the neutral (u_t and u_n , $u_t = (u_{ta} + u_{tb} + u_{tc})/3$) are shown in Fig. 5(a) and (b), respectively. The effective values of the fundamental (U_{1t} and U_{1n}) and third harmonic voltage



(a) Experimental results



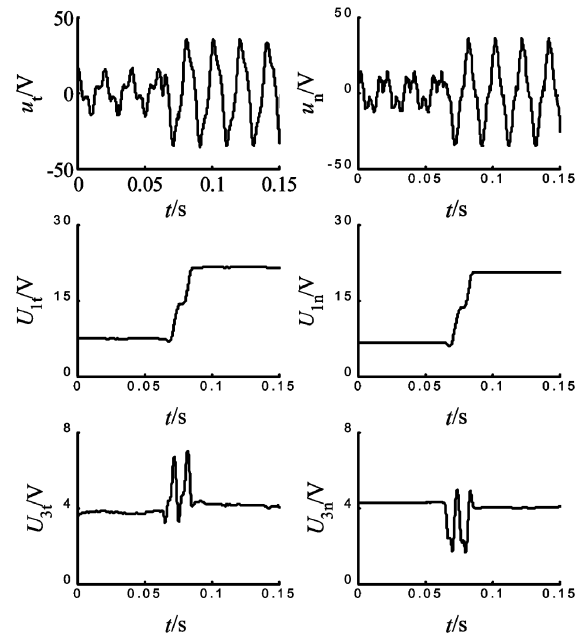
(b) Simulation results

Fig. 5. Zero-sequence voltages with solid ground fault (ungrounded neutral).

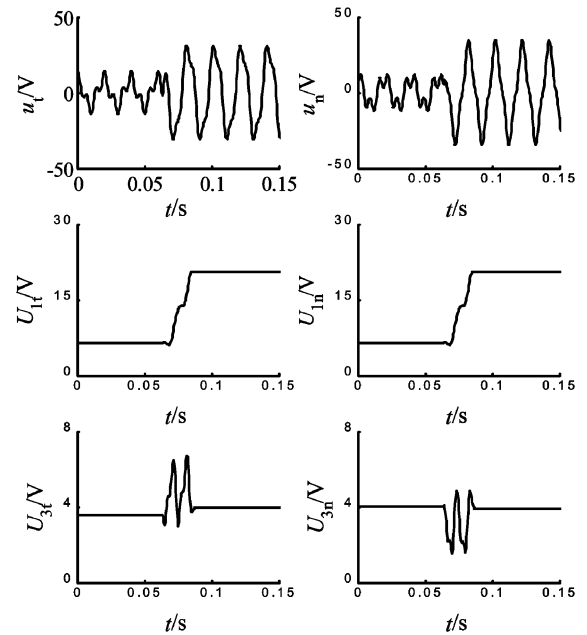
components (U_{3t} and U_{3n}) of u_t and u_n have also been calculated in real time by Fourier transform using a moving data window. Again, excellent agreement is achieved.

It is observed that before the ground fault occurs, the values of u_{3t} and u_{3n} are similar, while u_{1t} and u_{1n} are very small since the stator winding is symmetrical and the capacitances of the three phases a , b and c to ground are very similar, *viz.* 2.01 nF, 1.96 nF, and 2.11 nF, as mentioned earlier. After the fault, U_{3t} becomes higher than U_{3n} , while the changes in U_{1t} and U_{1n} are similar, which indicates that the zero-sequence fundamental frequency voltage can be extracted either at the generator terminals or at the neutral if it is to be used in the protection scheme.

In practice, the capacitance of each phase to ground is not as symmetrical as in the foregoing. To simulate the asymmetrical situation, three capacitances of 136.6, 107.8, and 106.4 nF are connected in parallel across the terminals of phases a , b , and c , respectively, and the neutral is grounded via a resistor



(a) Experimental results



(b) Simulation results

 Fig. 6. Zero-sequence voltages with ground fault via a resistance of 8.281 k Ω (the neutral is grounded via a resistance of 3.554 k Ω).

of 3.554 k Ω , and a ground fault is imposed at coil 2 of branch 1 of phase a through a transition resistance of 8.281 k Ω with the same excitation current of 7.7 A. This represents a typical high resistance fault condition, as might be simulated in order to assess the sensitivity of a protection scheme to detect such faults. The measured and simulated results for u_t and u_n and the corresponding components of the fundamental and third harmonic voltages are shown in Fig. 6(a) and (b), respectively. Under normal conditions, there is a higher fundamental frequency voltage at the neutral due to the asymmetrical distribution of the capacitances. The steady values of u_{3t} and u_{3n} are very small both before and after the occurrence of the fault, which means that the sensitivity of the protection would be low

for a ground fault with a high resistance if $U_{3t}/U_{3n} > 1$ is employed for the protection scheme.

V. CONCLUSIONS

Based on the multiloop circuit method, a comprehensive transient model has been established for predicting the current and voltage waveforms which results in a salient-pole synchronous generator when internal faults or ground faults occur on the stator winding. Good agreement has been achieved between simulated and measured results for both types of fault, and some important characteristics of the faults have been revealed. Thus, the model can be used to analyze the effects of various fault conditions on the stator windings, and to aid the design of protection schemes.

REFERENCES

- [1] V. A. Kinitzky, "Calculation of internal fault currents in synchronous machines," *IEEE Trans. Pattern Appl. Syst.*, vol. PAS-84, no. 5, pp. 391–389, May 1965.
- [2] —, "Digital computer calculation of internal fault currents in a synchronous machine," *IEEE Trans. Pattern Appl. Syst.*, vol. 87, no. PAS-8, pp. 1675–1679, Aug. 1968.
- [3] A. I. Megahed and O. P. Malik, "Synchronous generator internal fault computation experimental verification," *Proc. Inst. Elect. Eng., Gen. Transm. Distrib.*, vol. 145, no. 5, Sep. 1998.
- [4] —, "Simulation of internal faults in synchronous generators," *IEEE Trans. Energy Convers.*, vol. 14, no. 4, pp. 1306–1311, Dec. 1999.
- [5] P. P. Reichmeider, D. Querrey, C. A. Gross, D. Novosel, and S. Salon, "Partitioning of synchronous machine windings for internal fault analysis," *IEEE Trans. Energy Convers.*, vol. 15, no. 4, pp. 372–375, Dec. 2000.
- [6] —, "Internal faults in synchronous machines part I: The machine model," *IEEE Trans. Energy Convers.*, vol. 15, no. 4, pp. 376–379, Dec. 2000.
- [7] P. P. Reichmeider, C. A. Gross, D. Querrey, D. Novosel, and S. Salon, "Internal faults in synchronous machines part II: The model performance," *IEEE Trans. Energy Convers.*, vol. 15, no. 4, pp. 380–383, Dec. 2000.
- [8] M. Zilelichowski and M. Fulczyk, "Optimization of third harmonic ground-fault protection systems of unit-connected generators through neutralizer," *Elect. Power Syst. Res.*, vol. 45, pp. 149–162, 1998.
- [9] M. Fulczyk and J. Bertsch, "Ground-fault currents in unit-connected generators with different elements grounding neutral," *IEEE Trans. Energy Convers.*, vol. 17, no. 1, pp. 61–66, Mar. 2002.
- [10] —, "Neutral zero-sequence voltage in unit-connected generator for different grounding methods of generator neutral during fault in power system," in *Proc. 2001 5th Int. Power Engineering Conf.*, 2001, pp. 716–720.
- [11] N. L. Tai, X. G. Yin, and D. Chen, "Analysis of stator ground protection schemes for hydro-generator of three-gorges power plant based on zero sequence voltages," in *Proc. IEEE Power Engineering Society Winter Meeting*, vol. 3, 2000, pp. 1888–1893.
- [12] *Electromagnetic Transient Program (EMTP) Rule Book*, vol. 1 and 2, 1989.
- [13] *PSCAD/EMTDC Users Manual*, Manitoba HVDC Research Center, Winnipeg, MB, Canada, 1994.
- [14] J. D. Gao, X. H. Wang, and F. H. Li, *Analysis of Alternative Current Machine and its System* (in Chinese). Tsinghua, China: Tsinghua Univ. Press, 1994, pp. 1–43.
- [15] J. D. Gao and X. H. Wang, "The multi loop theory of alternating current machine and the analysis of internal faults laws of multi-branch windings," in *Proc. BICEM*, Beijing, China, 1987, pp. 202–205.
- [16] X. H. Wang, Y. G. Sun, B. Ouyang, W. J. Wang, Z. Q. Zhu, and D. Howe, "Transient behavior of salient-pole synchronous machines with internal stator winding faults," *Proc. Inst. Elect. Eng., Elect. Power Appl.*, vol. 149, no. 2, pp. 143–151, Mar. 2002.
- [17] X. H. Wang, S. L. Chen, W. J. Wang, Y. S. Guang, and L. Y. Xu, "A study of armature internal faults for turbogenerators," *IEEE Trans. Ind. Appl.*, vol. 38, no. 3, pp. 626–631, May/June 2002.
- [18] D. A. Calahan, "A stable accurate method of numerical integration for nonlinear systems," *Proc. IEEE*, vol. 56, pp. 744–744, 1968.



Daqiang Bi was born in Jilin Province, China, in 1973. He received the M.Sc. degree in electrical engineering from Shenyang University of Technology, Shenyang, China, in 1999, and the Ph.D. degree from Tsinghua University, Beijing, China, in 2003.

He is currently a post-doctoral Researcher at Tsinghua University. His research is mainly focused on the area of power system protection.



Xiangheng Wang was born in Anhui Province, China, in 1940. He graduated from the Department of Electrical Engineering in 1964 and received the Ph.D. degree in 1986, both from Tsinghua University, Beijing, China.

He was with Dongfang Electric Machine Works, Sichuan Province, China, from 1968 to 1978. He is currently a Professor at Tsinghua University, where he also conducts research on the analysis and control of electrical machines and systems, as well as their fault analysis and protection.



Weijian Wang was born in Jiangsu Province, China, in 1930. He graduated from the Department of Electrical Engineering, Tsinghua University, Beijing, China, in 1955.

He is currently a Professor in the Department of Electrical Engineering, Tsinghua University, where he is researching and teaching relay protection for large electric machine systems.



Z. Q. Zhu (M'90–SM'00) received the B.Eng. and M.Sc. degrees from Zhejiang University, Hangzhou, China, in 1982 and 1984, respectively, and was awarded the Ph.D. from the University of Sheffield, Sheffield, U.K., in 1991, all in electrical and electronic engineering.

From 1984 to 1988, he lectured in the Department of Electrical Engineering, Zhejiang University. Since 1988, he has been with the University of Sheffield, where he is currently Professor of Electronic and Electrical Engineering. His current major research interests include the application, control, and design of permanent magnet machines and drives.

Dr. Zhu is a Chartered Engineer and a Member of the Institution of Electrical Engineers (IEE), U.K.



David Howe received the B.Tech. and M.Sc. degrees from the University of Bradford, Bradford, U.K., in 1966 and 1967, respectively, and the Ph.D. degree from the University of Southampton, Southampton, U.K., in 1974, all in electrical power engineering.

He has held academic posts at Brunel University, Uxbridge, U.K., and Southampton University, and spent a period in industry with NEI Parsons Ltd. working on electromagnetic problems related to turbo-generators. He is currently Professor of Electrical Engineering at the University of Sheffield, where he heads the Electrical Machines and Drives Research Group. His research activities span most facets of controlled electrical drive systems, with particular emphasis on permanent magnet excited machines.

Dr. Howe is a Chartered Engineer, a Fellow of the Royal Academy of Engineering, and a Fellow of the Institution of Electrical Engineers (IEE), U.K.